SAND2018-14322J

The physics of irradiation of biological matter by ion beams.

M. A. Quinto[a], J. M. Monti[a], C. A. Tachino[a], P. F. Weck[b], O. A. Fojón[a], C. Champion[c], R. D. Rivarola[a]

[a] *Instituto de Física Rosario (CONICET-UNR), Rosario, Argentina*
[b] *Sandia National Laboratories, Albuquerque, USA*
[c] *CELIA, Bordeaux University, France*

Abstract

In radiobiology, predicting the evolution of irradiated biological samples still is nowadays an active field of research to identify DNA lesions or to adapt the radiotherapeutic protocols in radiation oncology. In this context, the numerical methods, based on Monte Carlo track-structure simulations, represent the most suitable and powerful tools for understanding the radiobiological damage induced by ionizing particles. However, most existing Monte Carlo track-structure codes require a large set of input data (cross sections) aiming at describing at the atomic scale the various particle-induced interactions in the medium of interest (water in liquid/vapor phase and DNA). In the present work, we report the theoretical differential and total cross sections, computed within a quantum mechanical continuum distorted wave-eikonal initial state (CDW-EIS) approach, for ion impact in water vapor and on DNA. These cross sections have been used to build up the input database for the homemade Monte Carlo track-structure *TILDA-V*. A comparison between the theoretical prediction and the available experimental data is presented. Micro-dosimetry results obtained with *TILDA-V* are also reported.

Keywords: Ion beams, Monte Carlo, Biological Matter

1. Introduction

Phenomena associated with radiation action in matter include a wide variety of physical, chemical and biological processes. It is nowadays well accepted that the nature of these interactions depends both on the type of radiation and on the impact energy. Besides, it is clearly known that the radiation process has a stochastic nature. Consequently, the numerical models, based on Monte Carlo (MC) approach, represent the most powerful tools that allow us to better understand the radiobiological damage induced by ionizing particles [1]. The MC approaches are used in various fields such as nuclear physics, astrophysics, plasma physics, solid state physics, accelerator driven system, radio-protection, radiobiology and medicine (radiotherapy and nuclear imaging). The MC methods developed for general purpose applications, known as condensed-history codes, are based on the macroscopic description of the particle transport. Among the most important ones, let us cite Geant4 [2], PHITS [3], FLUKA [4], MCNPX [5], EGS [6], which are used in high-energy physics, detector simulation, space radiation and medicine (see the review given by Nikjoo *et al.* [7]). However, in the ambit of micro-dosimetry, these general-purpose MC codes are generally not able to predict the radio-induced energy deposits at the nano-metric level and are therefore generally supplanted by MC track-structure (MCTS) approaches where the full particle histories are described interaction after interaction. It is noteworthy that the development of such event-by-event MCTS codes has been rather slower than the condensed-history codes, since requiring the building-up of a large set of input data (cross sections) aiming at describing at the atomic scale the various particle-induced interactions in the medium of interest (water in liquid/vapor phase and DNA). Besides, let us add that some existing codes also extend their scope to the simulation of the DNA damage induction by modeling the ensuing chemical stage (see for example [8, 9, 10]) and by considering specific DNA structure models [11, 10, 12, 13]. Generally speaking, all the MCTS codes devoted to the modeling of charged particle tracks in biological matter (ions, electrons and positrons) include input databases taken

from different standards (see for example [14, 15, 16]) and are mainly based on experimental data as well as semi-empirical approaches commonly used for dealing with the lack of available experiments. Drawing up an exhaustive list of models implemented into the MCTS codes documented in the literature would be a daunting task in view of the variety of existing approaches and we refer the interested reader to the dedicated references listed in table 1. Nevertheless, from a general standpoint, it is worth noting that the predictive power of such models remains either restricted to the domain of validity of theoretical approximations used or limited by the availability of the experimental data. Regarding the latter, we essentially find in the literature total cross sections, the multiple differential cross sections - needed to describe the angular and the energetic distributions of the secondary emitted electrons - being indeed rarely investigated due to the complexity of simultaneous energetic and angular detection. Therefore, semi-empirical laws are in general preferred in the numerical simulation of the transport process. However, the scarce measured data may occasionally produce arguable results that largely rely on extrapolations. Considering first the proton-induced ionization in water, the literature dedicated to MCTS codes focuses on two main models. The first one, denoted Rudd's model [17] was initially developed for protons impacting atomic and molecular targets. It provides an analytic equation for the energy distribution of electrons by means of a large set of fitting parameters deduced from experimental comparisons. It is based on a simple version of the binary-encounter approximation equation modified to yield the correct high-energy asymptotic dependence in agreement with the Bethe equation prediction and further modified by the use of the promotion model at low energies. In brief, the approximation made consists in treating the collision - between a projectile and a single target electron - as a classical one. The nucleus and the remaining target electrons play no other role that to provide a binding energy for the ejected electron. The justification for using a classical model lies in the fact that doubly differential cross sections for Coulomb scattering between two particles are the same when calculated using either classical physics or quantum mechanics. The second

semi-empirical and well-documented model - called HKS model since developed by Hansen, Kocbach and Stolterfoht [18] - consists in describing the ionization process within the impact parameter 1st Born approximation. In this approach, the initial and the final electron states are described by means of a hydrogenic function and a plane wave, respectively, i.e. without taking into account the electron momentum in its bound state. However, due to singularities observed when the ejected electron energy tends to zero, further empirical fittings were employed to finally provide the well-known HKS model [19]. When the proton energy becomes sufficiently low (< 100 keV/u), the ionization probability diminishes rapidly and the capture process becomes the predominant energy-loss pathway. However, to date, only rare experimental measurements have been reported for water. To overcome this lack, many semi-empirical simulations have been proposed for modeling the electron capture process. Let us cite the approach proposed by Rudd *et al.* [20], which consists in expressing the charge transfer cross section σ as $\sigma = \sigma_+ - \sigma_-$ by means of adjustable parameters for fitting the measured cross sections of positive (ion) and negative (electron) charge production (σ_+ and σ_-, respectively). The resulting cross sections agree well with the experimental data for proton energies of 1-100 keV but exhibit large discrepancies with the experimental measurements of Refs. [21, 22, 23]. More recently, Dingfelder *et al.* [24] suggested to express the charge transfer cross sections by analytical formula (straight lines for low and high proton energies on a doubly logarithmic scale, both connected by a power law) where the parameters were chosen by considering available experimental data.

Recently, other classical approximations based on the Classical Trajectory Monte Carlo (CTCM) have been used to investigate the interaction between incident ions and biomolecules. In this context, we find the works of Abbas *et al.* [25] and Lekadir *et al.* [26, 27], who have investigated the ionizing processes of ionization and single electron capture by using the CTCM - COB (Classical Over Barrier) potential for impacted of ions, namely, H^+, He^{2+} and C^{6+}, on water molecule and DNA nucleobases. The aforementioned ionizing processes have also been studied by Tran *et al.* [28] within a three-body CTCM,

where a set of total and differential cross sections have been computed. They found global agreement between theoretical and experimental results for C^{6+} impact on water molecule. In the same context, Illescas *et al.* [29] applied an independent-electron method combined with a classical trajectory MC approach to investigate the ionizing processes by impact of ions with water molecule in intermediate and high impact energy range. In particular, they focused on estimating cross sections for molecular fragmentation of water due to electron removal. Using the same argument, Nikjoo's group proposed a three-body CTMC method for calculating the probabilities of one-electron transitions [30]. They investigated the single and multiple electrons processes for carbon ions in the energy range of 1 - 10^4 keV/u impacting on molecular water. Using this method, they calculated a full set of total and differential cross sections to simulate the slowing-down of carbon ions (C^0-C^{6+}) with the KURBUC_carbon MTCS code [31]. Within a quantum-mechanical framework, Lüdde *et al.* [32] proposed a nonperturbative approach based on the basis-set-generator method (BGM). This method was applied to investigate ion collisions with water molecules, in particular ionization and electron capture by protons [32], multiple-electron removal by protons [33, 34] and He^+ [35], respectively, and by Li^{3+} ions [36]. The total cross sections predicted with BGM were in agreement with the experimental data. Also, the fragmentation channels resulting from multi-electrons removal were studied both theoretical and experimental.

In the context of perturbative quantum-mechanical method, a series of theoretical models to estimate the ionization as well as the electron capture cross sections for protons colliding with water molecules have been proposed [37, 38]. These models are based on either the 1st Born approximation with correct boundary conditions (CB1 model) or the continuum distorted wave-eikonal initial state approach (CDW-EIS model), the latter will be detailed in the following section. The CB1 model describes the active (ejected) electron as being in bound and continuum states of the target field in the entry and exit channel, respectively, while in the CDW-EIS approximation, a more complete representation of the active electron is introduced, considering that it evolves in the

simultaneous presence of the projectile and target fields in the entry and exit channels at all collision times, for single ionization as well as for single electron capture. Besides, these quantum-mechanical approach where recently used for describing the main ionizing processes induced by protons impacting on DNA nucleobasis (see [39, 40, 41] for ionization and electron capture, respectively). Recently, Quinto *et al.* used the CDW-EIS approximation to study the ionization and electron capture process induced by ions on molecular of biological interest [42, 43]. They computed a full set of total and differential cross sections to describe the slowing-down of protons in water and DNA biological medium with the *TILDA-V* MTCS code [44].

Other codes use CDW-EIS cross section databases, in particular for modeling the proton-induced ionization and capture processes: let us cite the work of Wiklund *et al.* [45] where light-ion beam secondary electron dose profiles in water were computed within the CDW-EIS framework and the recent LIonTrack code reported by Bäckström [46] where the CDW-EIS formalism is used to generate the initial energy and angle of secondary electrons emitted in ionizing collisions of light ions with H_2O molecules. Besides, it is worth noting that all these models were developed for modeling the proton transport in water considered in its vapor phase. Lately, many groups have investigated the transport of charged particles in liquid water and provided a theoretical approach of the proton-induced ionization processes (see for example [47, 24, 48]). In almost all cases, the cross sections are calculated within the plane wave Born approximation by taking into account a phenomenological dielectric-response function model deduced from reflectance measurements for modeling the liquid environment (see for example the recent work of [50]) and the review provided by Emfietzoglou *et al.* [51].

Modeling the full slowing-down of protons down to their neutralization in matter, namely, the Bragg peak region implies an accurate knowledge of all the inelastic interactions induced by the incident particle itself as well as its derivatives. Thus, in addition to the two above-discussed proton-induced ionization and electron capture, a MCTS code needs to describe the neutral-hydrogen-

induced ionization and electron-loss (stripping) processes. Unfortunately, these processes have been rarely investigated both theoretically and experimentally. Thus, to overcome the lack of available experimental measurements and theoretical support, semi-empirical approaches - mainly based on simple scaling and fitting rules - were preferred (see for example [24, 52]). Similarly, the excitation process induced by both protons and neutral-hydrogen atoms is commonly modeled by means of semi-empirical formulae [24, 52].

In this context, the present work will be focus on the theoretical prediction of cross sections for ionizing processes induced by ions on water molecule and DNA nucleobases. The theoretical cross sections will be compared with available experimental data. We will present some MTCS results obtained with the track-structure code *TILDA-V* [44]. *TILDA-V* (a French acronym for Transport d'Ions Lourds Dans l'Aqua & Vivo) is a code for modeling heavy ion and secondary electron histories in vapor water for impact energies ranging from 10 keV/u to 100 MeV/u. This current version is based on a complete set of quantum-mechanically calculated multiple differential and total cross sections to describe all the inelastic processes occurring throughout the slowing-down of protons in water and DNA components (adenine (A), thymine (T), cytosine (C), guanine (G) and sugar phosphate (SP) backbone).

2. Theory

Let us consider an incident ion of charge Z_P impacting on a neutral target, Z_T, with a velocity $\mathbf{v}$. If the impact velocities considered are high enough, we can admit that the times associated with the vibration and rotation of the target are much larger than the characteristic times of the collision. Besides, it is also possible to assume that the target nuclei remain fixed in their initial positions during the reaction. With respect to the multi-electronic problem, it is reduced to the analysis of a one-active electron system by considering that all the other electrons (the passive ones) remain frozen in their initial orbitals during the collision and that the active electron evolves independently of them

Table 1: Monte Carlo track-structure codes for radiation research at cellular level

Code	Incident Beam	Energy range	Medium	References
DELTA	protons, α particles	0.3 MeV/u - 4 MeV/u	water (liq, vap)	[53]
	electrons	10 eV - 10 keV		
KURBUC	protons	1 keV - 300 MeV	water (liq)	[54, 55]
	α particles	1 keV/u - 2 MeV/u	water (liq)	[56]
	carbon ions	1 keV/u - 10 MeV/u	water (liq)	[31]
LIonTrack	ions	1 MeV/u - 300 MeV/u	water (liq)	[46]
GEANT4-DNA	ions	1 keV/u - 400 MeV/u	water (liq)	[57]
	electrons	7.4 eV - 1 MeV		
Kramer & Kraft	ions	20 keV/u - 100 MeV/u	water (liq)	[58]
MC4	ions	$>$ 0.3 MeV/u	water (liq, vap)	[59]
	electrons	$>$ 10 eV		
MOCA14	proton, α particles	0.3 MeV/u - 4 MeV/u	water (vap)	[60]
NOTRE DAME	ions	$>$ 0.3 MeV/u	water (liq, vap)	[61]
	electrons	$>$ 10 eV		
OREC	ions	0.3 MeV/u - 4 MeV/u	water (liq)	[62]
	electrons	10 eV - 1 MeV		
PARTRAC	ions	0.3 MeV/u - 1 GeV/u	water (liq,vap)	[24]
	electrons	8.2 eV - 10 MeV		
Penelope	ions	10 keV/u - 10 GeV/u	various	[63]
	electrons, positron	100 eV - 10 GeV		
PITS	ions	0.3 MeV/u - GeV/u	biological	[64]
	electrons	$>$ 10 eV		
SHERBROOKE	ions	$>$ 0.3 MeV/u	water (liq,vap)	[65]
	electrons	$>$ 10 eV		
TILDA	ions	10 keV/u - 100 MeV/u	water (liq,vap)	[66]
TILDA-V	protons	10 keV - 100 MeV	water (liq,vap) DNA-nucleobases	[44]
	electrons	7.4 eV - 300 keV		

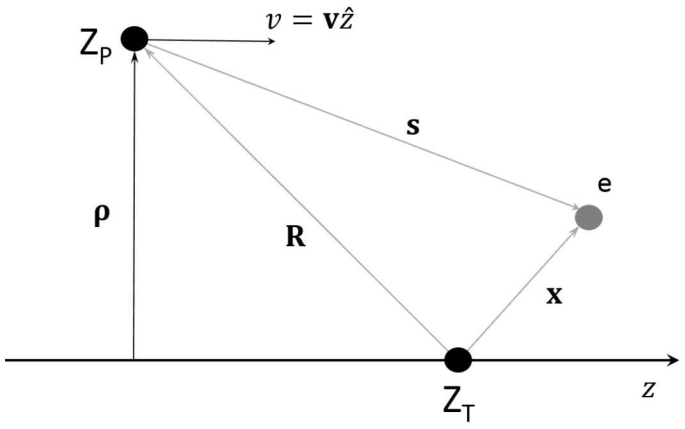

Figure 1: Coordinate system in the impact parameter approximation

in an effective mean field of the residual target. This approximation was first formulated with success to study electron capture [67] and ionization [68] (see also Refs. [69, 70] for the case of atomic targets). It was then extended to molecular targets for both reactions, electron capture [71] and ionization [72]. Therefore, within the independent electron model and considering that there is just one active electron, the multi-electronic Hamiltonian of the collision system can be described as

$$H_{el} = -\frac{1}{2} \bigtriangledown^2 + V_T(\mathbf{x}) + V_P(\mathbf{s}) + V_s(\mathbf{R}) \tag{1}$$

where $\mathbf{x}$ ($\mathbf{s}$) is the active electron coordinate in the target (projectile) reference frame, $V_T(\mathbf{x})$ is an effective one-electron target potential, $V_P(\mathbf{s})$ is the interaction between the projectile and the active electron, and $V_s(\mathbf{R})$ is the interaction of the projectile with the target nuclei and the passive electrons (see fig. 1). This last potential depends only on the internuclear coordinate $\mathbf{R}$ and thus, within the straight-line version of the impact-parameter approximation gives rise to a phase factor which only affects the projectile scattering [68]. Consequently, we will drop this term, as we are not interested in the angular projectile distribution.

We opt for solving the collisional problem within the CDW-EIS approximation that was introduced by Crothers and McCann to investigate the single

ionization of H by bare ion impact [73]. The CDW-EIS approximation was proposed to improve the large overestimation of the total cross sections, at intermediate impact energies obtained with the Continuum Distorted Wave (CDW) model [74], which stems from the lack of normalization of at least one of the distorted wave functions in the initial and final channels [75]. This approximation solves the aforementioned problem, both for single ionization and single electron capture and exhibits, in general, a very good agreement with existing experimental data for differential and total cross sections. The scattering amplitude as a function of the impact parameter in the *prior*-version within CDW-EIS approximation can be written as:

$$\mathcal{A}_{if}^{-}(\boldsymbol{\rho}) = -i \int_{-\infty}^{+\infty} dt \left\langle \chi_f^- \left| \left[\left(H_{el} - i\frac{\partial}{\partial t} \right) \right| \chi_i^+ \right\rangle \right] \tag{2}$$

where χ_i^+ and χ_f^- are the initial and final distorted wavefunctions, respectively. The distorted wavefunction χ_i^+ does not contribute to the transition amplitude as $t \to +\infty$. By employing the Fourier transform, $\mathcal{A}_{if}^-$ can be expressed as a function of the transverse momentum transfer $\boldsymbol{\eta}$:

$$\mathcal{R}_{if}^{-}(\boldsymbol{\eta}) = \int d\boldsymbol{\rho} \exp(i\boldsymbol{\rho}.\boldsymbol{\eta}) \mathcal{A}_{if}^{-}(\boldsymbol{\rho}) \tag{3}$$

2.1. Bare ion ionization

In the CDW-EIS approximation, the initial and final distorted wave functions for the ionization process can be written as

$$\chi_i^+(\boldsymbol{x}, \boldsymbol{s}, t) = \Phi_i(\boldsymbol{x}, t)\, \mathcal{L}_i^+(\boldsymbol{s}) \tag{4}$$

$$\chi_f^-(\boldsymbol{x}, \boldsymbol{s}, t) = \Phi_f(\boldsymbol{x}, t)\, \mathcal{L}_f^-(\boldsymbol{s}) \tag{5}$$

In equations (4) and (5), the terms $\Phi_i(\boldsymbol{x}, t) = \phi_i(\boldsymbol{x}) \exp(-i\varepsilon_i t)$ and $\Phi_f(\boldsymbol{x}, t) = \phi_f(\boldsymbol{x}) \exp(-i\varepsilon_f t)$ are the initial and final wave functions, respectively, solutions of the time-dependent Schrödinger equation. ε_i is the electron energy of a target orbital and ε_f is the electron energy in the final state. The terms $\mathcal{L}_i^+(\boldsymbol{s})$ and $\mathcal{L}_f^-(\boldsymbol{s})$ represent the initial and final distortion functions, respectively. The initial bound wave function of the active electron, $\phi_i(\boldsymbol{x})$, is approximated by

a Roothaan-Hartree-Fock wavefuncion (for more details see Appendix of Ref. [76]). Whereas, in the final channel the active electron wavefunction is given by

$$\phi_f(\boldsymbol{x}) = \frac{1}{(2\pi)^{3/2}} \exp\left(i\,\boldsymbol{k}\cdot\boldsymbol{x}\right)\; N^*(\lambda)\,{}_1F_1\left[-i\,\lambda, 1, -i\;(kx + \boldsymbol{k}\cdot\boldsymbol{x})\right] \tag{6}$$

with $\varepsilon_f = k^2/2$ is the final electron energy,$\boldsymbol{k}$ being the ejected electron momentum in the target reference frame. The term $N(a) = \exp(\pi a/2)\Gamma(1-ia)$ (with Γ being the Euler's Gamma function) is the normalization factor of the ${}_1F_1$ hypergeometric function, and $\lambda = \tilde{Z}_T/k$ with $\tilde{Z}_T$ an effective charge. This charge is chosen in correspondence with the energy of the target orbital as $\tilde{Z}_T = \sqrt{-2n^2\varepsilon_i}$, with n being the principal quantum number of the target orbital [77].

In the CDW-EIS approximation, the initial distortion is defined as follows

$$\mathcal{L}_i^+(\boldsymbol{s}) = \exp\left[-i\nu\ln(vs + \boldsymbol{v}\cdot\boldsymbol{s})\right] \tag{7}$$

whereas, the final distortion is written as

$$\mathcal{L}_f^-(\boldsymbol{s}) = N^*(\zeta)\,{}_1F_1\left[-i\zeta; 1; -i\;(ps + \boldsymbol{p}\cdot\boldsymbol{s})\right] \tag{8}$$

where $\boldsymbol{v}$ is the projectile velocity, $\nu = Z_P/v$, $\zeta = Z_P/p$ and $\boldsymbol{p} = \boldsymbol{k} - \boldsymbol{v}$ is the ejected electron momentum in the projectile reference frame.

Finally, the double differencial cross section for ionization, by bare projectiles, is obtained as,

$$\frac{\partial\sigma_{if}^2}{\partial E_k \partial\Omega_k} = k\int d\boldsymbol{\eta}|\mathcal{R}_{if}^-(\boldsymbol{\eta})|^2 \tag{9}$$

2.2. Dressed ion ionization

Recently Monti and co-worker [78] have extended the CDW-EIS and CDW approximations to the case of dressed projectiles. The authors have considered the effect of the projectile passive electrons at the same level as the target passive electrons. Thus, they have assumed that the projectile electrons screen the projectile nuclear charge and that the interaction between the screened projectile and the active electron can been described by a model potential. The latter, $V_P(\boldsymbol{s})$, has been described by an analytic independent-particle model

potential given by Green *et al.* [79], which is usually called the Green-Sellin-Zachor (GSZ) potential. This potential can be written as a long-range term plus a short-range term due to the asymptotic screened projectile charge q:

$$
\begin{aligned}
V_a(s) &= -\frac{q}{s} \\
V_s(s) &= -\frac{1}{s}(Z_P - q)[H(\exp(s/d) - 1) + 1]^{-1} \\
V_P(s) &= V_a(s) + V_s(s)
\end{aligned}
$$

with H and d being adjustable parameters [79, 80]. The first term, $V_a(s)$, corresponds to the asymptotic Coulomb potential due to the projectile asymptotic charge q and the second one, $V_s(s)$, gives a short-range potential due to the electrons in the dressed projectile. The main use of these potentials is that values of the parameters H and d exist for many ions in different charge states. The variation of these parameters is relatively smooth and they can be obtained for many more dressed ions by interpolating or extrapolating the available ones.

For dressed ions, the initial and final states are the same as those defined by Eqs. (4) and (5) previously described in case of ionization by bare projectile. Therefore, when the additional short-range potential is introduced in the scattering amplitude given by Eq. (2), it gives place to a new term:

$$
\mathcal{A}_{if}^{-(s)}(\boldsymbol{\rho}) = \int_{-\infty}^{+\infty} dt \, \langle \chi_f^- \, | V_s(s) | \, \chi_i^+ \rangle \tag{10}
$$

Thus, the final scattering amplitude is now expressed as the contribution of two terms: the first one representing the asymptotic Coulomb contribution and the second one describing the short-range correction [78].

$$
\mathcal{A}_{if}^{-}(\boldsymbol{\rho}) = \mathcal{A}_{if}^{-(a)}(\boldsymbol{\rho}) + \mathcal{A}_{if}^{-(s)}(\boldsymbol{\rho}) \tag{11}
$$

Finally, the double differential cross section for ionization, by dressed projectiles, is obtained through Eq. (9) where the $\mathcal{R}_{if}^{-}(\boldsymbol{\eta})$ is given by

$$
\mathcal{R}_{if}^{-}(\boldsymbol{\eta}) = \mathcal{R}_{if}^{-(a)}(\boldsymbol{\eta}) + \mathcal{R}_{if}^{-(s)}(\boldsymbol{\eta}) \tag{12}
$$

2.3. Bare ion electron capture

The CDW-EIS approximation was introduced to investigate the electron capture by Martinez and co-workers [81]. This approximation was extensively used to predict the electron capture process for various systems. In the work of Ref. [72], the CDW-EIS approximation was used to predict TCS of biological molecules by proton impact. Also, Champion *et al.* reported electron capture cross section of DNA nucleobases impacted by proton beams [41]. Recently, Quinto *et al.* used this method to investigate the electron capture process for molecules of biological interest impacted by high charged ions [43]. In these works, a good agreement of the CDW-EIS results with the experimental data was found at medium and high impact energies.

For electron capture, the initial distortion wave function, $\chi_i^+(\boldsymbol{x}, \boldsymbol{s}, t)$, remains unchanged with respect to the case of ionization (see equation (4)). On the other hand, the final distortion wave function is considered as:

$$\chi_f^-(\boldsymbol{x}, \boldsymbol{s}, t) = \Phi_f(\boldsymbol{s}, t)\, \mathcal{L}_f^-(\boldsymbol{x}) \tag{13}$$

where $\Phi_f(\boldsymbol{s}, t) = \phi_f(\boldsymbol{s}) \exp(-i\varepsilon_f t + i\boldsymbol{v}\cdot\boldsymbol{x} - i\frac{v^2}{2}t)$ is the final projectile state and ε_f is the corresponding electron energy. $\phi_f(\boldsymbol{s})$ is the corresponding hydrogenic function with charge Z_P describing the final bound state.

The final distortion is chosen as:

$$\mathcal{L}_f^-(\boldsymbol{x}) = N^*(\xi)\, {}_1F_1\left[-i\xi; 1; -i\ (vx + \boldsymbol{v}\cdot\boldsymbol{x})\right] \tag{14}$$

with $\xi = \tilde{Z}_T/v$, whereas the active electron final state, $\phi_f(\boldsymbol{s})$, is ahydrogenic projectile bound state with charge Z_P and energy $\varepsilon_f = -Z_P^2/(2n_P^2)$, with n_P being its principal quantum number. The total cross section for electron capture is given by,

$$\sigma_{if} = \int d\boldsymbol{\eta} |\mathcal{R}_{if}^-(\boldsymbol{\eta})|^2 \tag{15}$$

3. Charged particle transport

Monte Carlo charged particle transport simulation comprises series of sampling steps, which first determine the distance λ between two successive inter-

actions. The latter is selected by assuming that the charged particle transport in matter is governed by a Poisson law $p(\lambda)$, whose corresponding probability $P(\lambda)$ is defined by:

$$P(\lambda) = \int_0^{\lambda} du\, p(u) = 1 - \exp\left(\frac{-\lambda}{\tilde{\lambda}}\right) \tag{16}$$

This probability is usually sampled by means of pseudorandom variables defined in the interval $[0;1]$, namely, $\Gamma \equiv \Gamma(0;1)$, that finally leads to a distance λ given by

$$\lambda = -\tilde{\lambda}\ln(1-\Gamma) = -\tilde{\lambda}\ln(\Gamma') \quad \text{with} \quad \Gamma' \equiv \Gamma'(0;1) \tag{17}$$

In equation (16), $\tilde{\lambda}$ refers to the mean free path defined as $\tilde{\lambda} = 1/(n\sigma_T)$, where n denotes the number of target molecules per volume unit defined as $n = N_A \times \rho/A_{mol}$, where N_A is Avogadro's number, ρ and A_{mol} are the density (in g.cm^{-3}) and the molar mass of the crossed medium, respectively, and σ_T is the total cross section including all the interactions considered for modelling the transport of the particle of interest. In its current version, *TILDA-V* takes into account the following collisional processes: - for protons: elastic scattering, ionization, capture and excitation; - for neutral-hydrogen atoms: elastic scattering, ionization, electron loss (stripping) and excitation; - for secondary electrons elastic scattering, ionization and excitation. The kinematics of the interaction is determined by the multiple differential cross sections of the corresponding process. For example, if the selected process is ionization or stripping, singly and doubly differential cross sections are successively used to determine both the kinetic energy and the emission angle of secondary electron. Then, the incident particle energy is reduced by the total energy (kinetic + potential) transferred during the collision. Besides, the charge exchange of the proton particle is taken into account. Thus, when an electron capture occurs the proton charge decreases, as results a neutral hydrogen primary particle is recovered. Whereas, when an electron loss process (stripping) occurs, the neutral hydrogen charge increases, leading to the creation of a primary proton particle. All the secondary electrons emitted during the various ionizing processes (ionization, electron loss), induced by H^+ and/or H^0 impact, are followed step-by-step with

the MCTS code EPOTRAN (an acronym for Electron and Positron Transport in liquid and vapor water) [82]. All these steps are repeated for all primary and secondary particles until their kinetic energy falls below a predetermined cut-off value. For the primary particles, namely, proton and hydrogen, the cut-off energy is fixed at 10 keV, while for the secondary electrons the latter is fixed at 7.4 eV. When an ionization or capture process occurs on inner-shells, the vacancy may be accompanied by non-radiative transitions, including the emission of Auger as well as Coster-Krönig electrons. These processes are considered in *TILDA-V* for all the investigated targets, namely, by considering both the probability and the corresponding electron energy. For water, we adopted the data reported in Martin's thesis [83], while for DNA the Auger electron non-radiative probabilities and energies provided by the Livermore Evaluate Atomic Data Library [84] are used for the different atomic constituents involved in the biomolecular target description [44].

4. Biological matter description

In the case of describing the biological matter by water or through the basic DNA components (A, C, T, G and SP), the biological medium has been modeled by using molecular wave functions, all obtained on quantum mechanical grounds. The description of the initial ground state molecular orbitals are assumed to be obtained by linear combinations of atomic orbitals (LCAOs) approximation. Thus, the initial bound state of a molecule, ϕ_i, can be represented by a linear combination of Slater-type functions, namely,

$$\phi_i = \sum_{k=1}^{N_s} \alpha_k \varphi_k, \tag{18}$$

N_s being the number of Slater functions that composed the atomic orbital and φ_k defined as,

$$\varphi_k(\boldsymbol{r}) = R_k(r) Y_l^m(\hat{r}) \tag{19}$$

where $R_k(r)$ is the radial part given by

$$R_k(r) = \frac{(2\mathcal{Z}_k)^{n+1/2}}{\sqrt{(2n)!}} r^{n-1} e^{-\mathcal{Z}_k r} \tag{20}$$

The coefficients α_k and $\mathcal{Z}_k$ are tabulated for various atoms in Ref. [85] and the angular part $Y_l^m(\hat{r})$ represented by spherical harmonics. For more details about the initial state active electron description we refer the reader to our previous work [76].

Finally, the cross section for a given molecular orbital is obtained by summing up the contribution of each atomic cross section that correspond to a given molecular orbital,

$$\sigma_j = \sum_{i=1}^{N_i} \beta_{j,i} \sigma_i \tag{21}$$

with σ_i the atomic cross section, which is computed using Eq. (9) for ionization and Eq. (15) for electron capture, respectvely, $\beta_{i,j}$ being the effective electron occupation number and N_i is the number for a given molecular orbital. For water, the corresponding binding energies, ϵ_i are computed by employing a self-consistent field method (MO-LCAO-SCF), whereas a complete neglected of differential overlap (CNDO) approximation is employed for the effective occupation electron analysis of the different molecular orbitals [86]. Regarding the DNA components, an *ab initio* method in which all the molecular orbitals of each DNA component were described by a linear combination of atomic wave functions by using the GAUSSIAN09 software at the RHF/3-21G level [87] was adopted. For more details, we refer the interested reader to our previous study [40] where the CNDO descriptions of DNA nucleobases, including the binding energies and the effective electron occupation, needed to describe the target molecular wave functions are reported. Let us mention that the biomolecular targets under investigation are considered as isolated molecules and refer to living matter components in vapor state. In this sense, this work clearly differs from the existing studies on liquid water and/or condensed DNA where the energy-loss function of realistic biological components was extracted from

experimental data and interpolated for use in cross section calculations (see for example the series of works provided by Abril and co-workers[88, 89]).

Finally, in order to gain insight into the real energy deposit cartography induced by proton impact in biological medium, we have considered a typical nucleotide i.e. an equivalent unit of DNA molecule composed of a nucleobase-pair plus two SP groups [90]. Additionally, to fit the realistic composition of living cells, we also took into consideration the nucleobase repartition percentages reported by Tan *et al.* [91], namely, 58% (A-T) (adenine-thymine base pair) and 42% (C-G) (cytosine- guanine base pair). However, this description refers to dry DNA, which obviously cannot mimic the biological reality, mainly composed of hydrated DNA. Thus, starting from the work of Birnie *et al* [92], who estimated that the total amount of water associated with DNA was of the order of 50 moles per mole of nucleotide, in order to get the expected density of 1.29 g.cm^{-3}, we have considered a biological medium composed of hydrated DNA by adding 18 molecules per nucleotide. As a result, the final nucleotide has a mass equal to 947.87 g.mol^{-1} with the following mass percentages: A (8.3%), T (7.7%), C (4.9%), G (6.7%), SP group (38.1%) and water (34.3%) [93]. Thus, when particles cross hydrated DNA, a random sampling, based on the mass percentage, is used for precisely selecting the DNA component impacted [44].

5. Results

In this section we will present the results of theoretical calculation obtained within CDW-EIS approximation and a comparison with experimental data will be done where possible. Moreover we will show some outcomes of *TILDA-V* MCTS code.

5.1. Theoretical cross sections

In Figs. 2 and 3, we report the DDCS obtained within CDW-EIS approximation for different ions, H^+, He^{2+}, C^{4+}, and O^{8+}, respectively, impacting on water molecule. In general, we observe a good agreement between the CDW-EIS

calculations and the measurements for the different emission angles presented. In general, for the different presented projectiles type, we can observe a good agreement of the DDCS, as a function of the electron ejected energy, with the experimental data, for various emission angles. In Figs. 2(b) and 3, the CDW-EIS results underestimated the DDCS in backward angle emission for an ejected energy greater that some hundreds eV. In Fig. 3, we can observe in the measurements, the contributions of K-LL Auger peaks of oxygen, which were clearly observed at around 480 eV for all angles. In particular, for the C^{4+}, the experimental DDCS at 30 degrees, present the electron loss to the continuum peak (ELC) around 3 keV and the binary peak around 10 keV. The latter is also well described by the theoretical calculations. Whereas, both Auger emission and ELC contribution are not included in the theoretical model. In Fig. 4 we present the theoretical DDCS results computed within CDW-EIS approximation for H^+ and C^{6+} ions impacting on adenine and uracil molecules, respectively. For adenine molecule, we have a good agreement between the theoretical DDCS and experimental data. However, we can observe the CDW-EIS results underestimate the measurement for backward (135 degrees) angle. Also, slight discrepancy is found for low ejected energy, less that a hundred eV, for forward angle emission (15 degrees). Besides for adenine ($C_5H_5N_5$), reported measurements, two peaks appears at approximately 250 and 400 eV, these are K-LL Auger electrons contribution from carbon and nitrogen atoms, respectively. For uracil molecule, the CDW-EIS results describe well the experimental data in the presented energy range. Similarly to the case of adenine, the uracil, ($C_4H_4N_2O_2$), experimental DDCS present an extra K-LL Auger electrons contribution at around 480 eV given by the oxygen.

In Fig. 5, we present the total cross sections (TCS) for electron ionization and electron capture of vapor water molecule impacted by, H^+, He^{2+} and C^{6+} ions, as a function of the incident energy. For all of them a good agreement with experimental data is found in almost all the presented energy range. In the case of electron ionization by C^{6+}, only one experimental result is available in the literature, which is obtained as a result of the numerical integration of DDCS

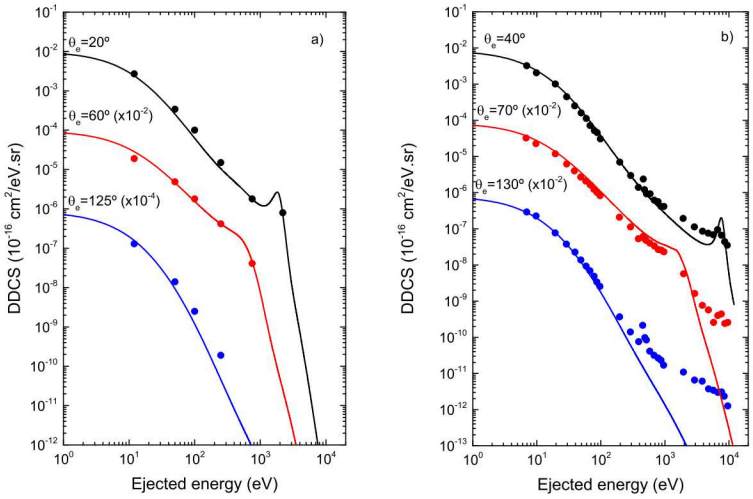

Figure 2: (Color online) CDW-EIS calculations of double differential cross sections of water impacted by 1 MeV proton (panel a) and 6 MeV/u He^{2+} (panel b). Experimental data are taken from [94] (panel a) and from [95] (panel b).

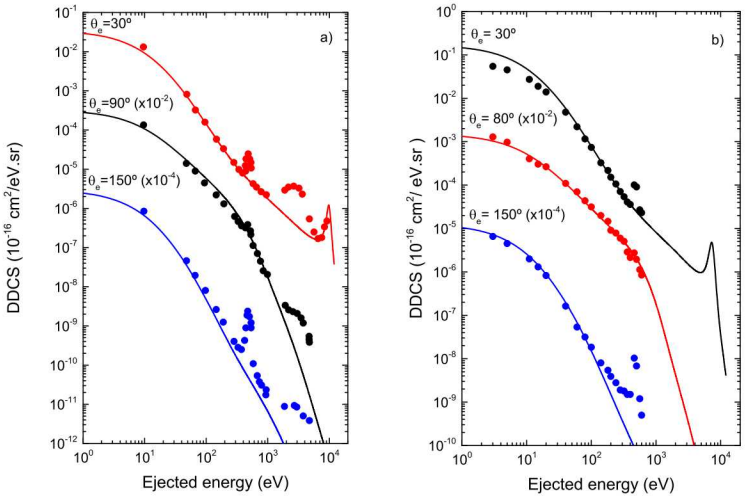

Figure 3: CDW-EIS calculations of double differential cross sections of water impacted by 6 MeV/u C^{4+} (panel a) and 4.5 MeV/u O^{8+} (panel b). Experimental data are taken from [96] (panel a) and from [97] (panel b).

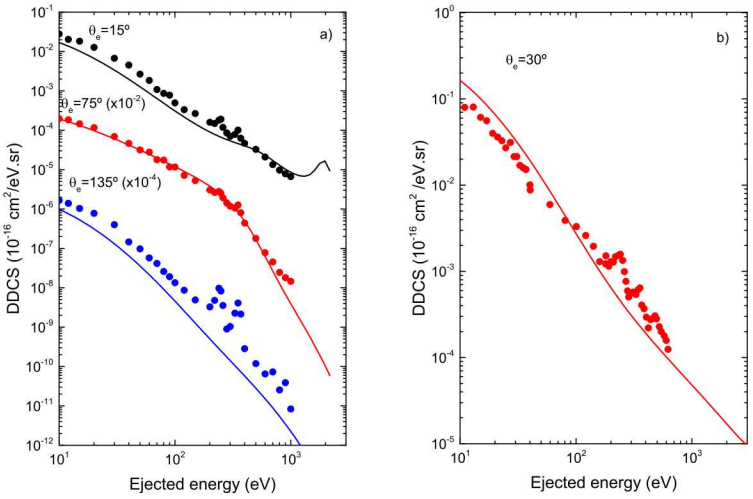

Figure 4: CDW-EIS calculations of double differential cross sections of adenine molecule impacted by 1 MeV proton (panel a) and uracil molecule impacted by 3.5 MeV/u C^{6+} (panel b). Experimental data are taken from [98] (panel a)and from [99] (panel b).

[106]. Besides, no experimental data are available for electron capture. We must also indicate that the theoretical calculations overestimate the experimental data at collision energies lower than 150 keV/u for alpha particle impact.

5.2. TILDA-V results

In this section we will present some radiodosimetry results obtained with *TILDA-V* code [44]. We report the dose profile computed in water as well in hydrated DNA medium. To do that, we have followed the procedure proposed by Wiklund *et al.* [45], which consists in subdividing the proton track in cylindrical shells with a logarithm size (33 bins in radial range from 0.1 nm to 240 nm) and scoring all the secondary electron histories along a 40μm proton track. The results for 1 MeV proton are presented in Fig. 6, along with a selection of previous MC results and analytical calculations. Experimental data taken from Wingate and Baum [108] are also reported. Our simulations (red stepped line) are consistent with Wiklund *et al.*'s results (green stepped line) even at small radius ($<$ 1 nm), which stems from the fact that their MC code is based

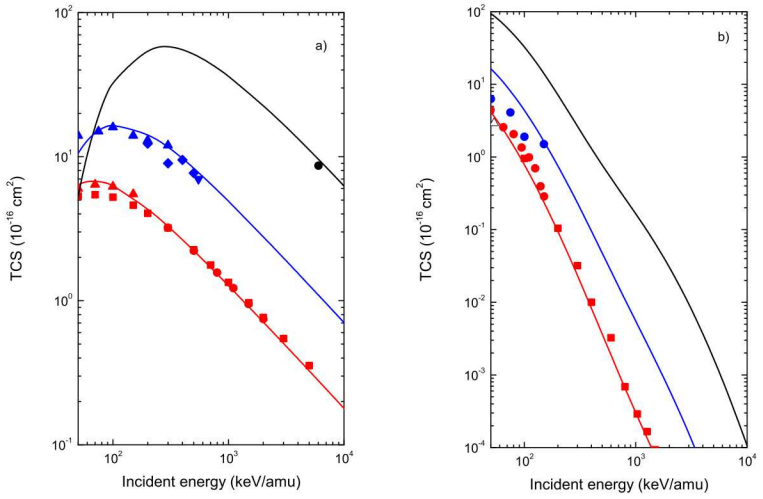

Figure 5: CDW-EIS calculation of total cross sections of water impacted by ions: red line, H^+; blue line, He^{2+}; and black line, C^{6+}; (panel a) ionization and (panel b) electron capture. Experimental data are taken from [100] red squares, [101] red circles , [102] red up triangles, [103] blue diamonds, [104] blue up triangles, [105] blue down triangles, [106] black circle (panel a) and from [23] red squares, [107] red circles blue, [103] circles (panel b).

on a similar CDW-EIS theory than ours for treating the secondary electron emission. Only small differences can be seen, which are due to the variant of secondary particle tracking performed using the PENELOPE code in the work of Wiklund *et al.* [45]. At large distances the data reported by Wiklund *et al.* slightly tend to overestimate our calculations. The LionTrack profile (blue line) largely underestimates our results as well as the experimental data for $r < 1$ nm, whereas it tends to overestimate the data for higher radii. This disagreement is particularly surprising since the CDW-EIS model is also employed for describing the proton-induced ionization process as well as the PENELOPE code for modeling the secondary electron tracks. However, the authors indicated that the input dataset used for tracking the secondary electrons in their simulations was Dingfelder's database cross sections [46, 47], whereas the default PENELOPE database was used in the work of Wiklund *et al.*. The profiles provided by Olko *et al.* based on MOCA-14 track-structure code (magenta stepped line)

by Emfiezoglou *et al.* based on MC4V track-structure code (orange stepped line) with the dielectric response model and by Wilson *et al.* based on PITS track-structure code (violet stepped line) appear overestimated, in particular in the low-radius domain ($r < 1$ nm), while they converge to our results at higher distances. Finally, a large degree of similarity is observed between our profile and the calculations of Olivera and co-workers [109], while the prediction by Butts and Katz [110] and the semi-analytical calculation reported by Wiklund *et al.* [45] overestimate all the profile up to 10 nm from the ion track.

We report a study, made with the MTCS *TILDA-V* code, on the influence of the theoretical approximation used to compute the ejected angle of the secondary particle for the ionization process induced by proton on water. The results shown in Fig. 7, both profiles have been computed for an incident proton energy of 100 keV and 1 MeV. In the Bragg's peak region, the radial profiles, obtained with both theoretical approaches, present a discrepancy for low radii (< 1 nm). Whereas, for a radii greater than 1 nm, both profiles show the same trend. For 1 MeV incident proton energy, neither profiles present a notable difference. Thus, we can deduce that the importance of the quantum-mechanical model is most relevant in the low energy, in particular in the Bragg's peak region. Also, we investigated the influence of the biological medium description on the radial dose profile for protons beam energy of 100 keV and 1 MeV. In a first attempt, we used the vapor water to characterize the biological matter and then the hydrated DNA, with density of 1 g.cm^{-3} and 1.29 g.cm^{-3}, respectively. The results are depicted in Fig. 6, for both incident proton energies, the hydrated DNA profile is approximately 1.5, close to the ion track, greater than water one. Besides, we can observe that this gap is not constant in all the presented radii, it seems to decrease as the radial profile increase. In fact, the profiles intersect nearly to radius of 2 nm, after that the water profile dominates the hydrate DNA one for large radii.

In Fig. 9, we report a micro-dosimetry calculations, made with *TILDA-V*, of proton depositing energy in cylinders (height $\times$ radius) of 2×1 nm, 10×2.5 nm and 25×12.5 nm. We choose these dimensions since they represent the ge-

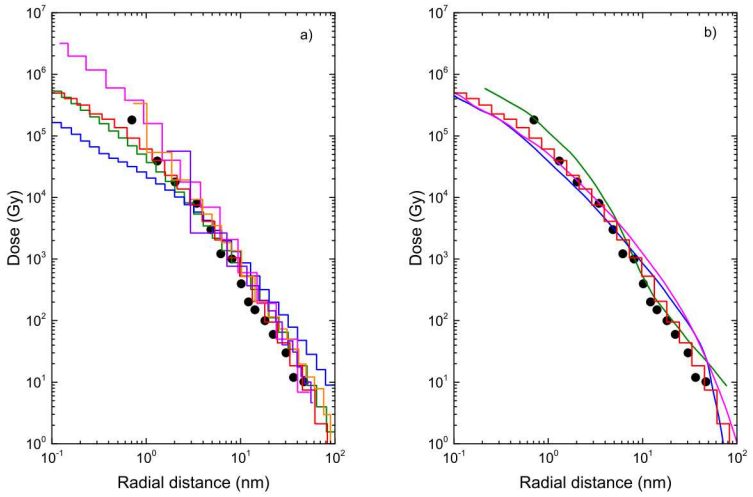

Figure 6: Radial dose profile Monte Carlo results stepped line: red, *TILDA-V*; green, MC [45]; blue, LIonTrack [46]; magenta, MOCA-14 [111]; orange, MC4V [112]; violet PITS [64] (panel a). Comparison of *TILDA-V* results (stepped red line) with analytical ones solid lines: blue, [109]; green [110]; magenta [45] (panel b). Experimental data: circles [108].

ometrical model of DNA segment, nucleosome and chromatin fibre, respectively. The simulations are carried out considering a random trajectory of the proton beam incident on the cylinder, which containing either vapor water or hydrated DNA with density 1 g.cm^{-3} and 1.29 g.cm^{-3}, respectively. As shown in Fig. 9, we observe a peak of deposit energy, both for the primary and secondary particles, protons and electrons, respectively. This peak move toward high energy as the dimensions of the cylinder increase. Besides, in the left part of the peak, we observe that the deposit energy by protons is greater in cylinder filled with water then in those filled with hydrated DNA. Whereas, in the case of deposit energy by secondary electrons, it is always more significant for cylinders filled with hydrated DNA that those filled with water.

6. Conclusions

To sum up, in this work we described the main points of the physics of irradiation of living matter by charged particles. In particular, we given an

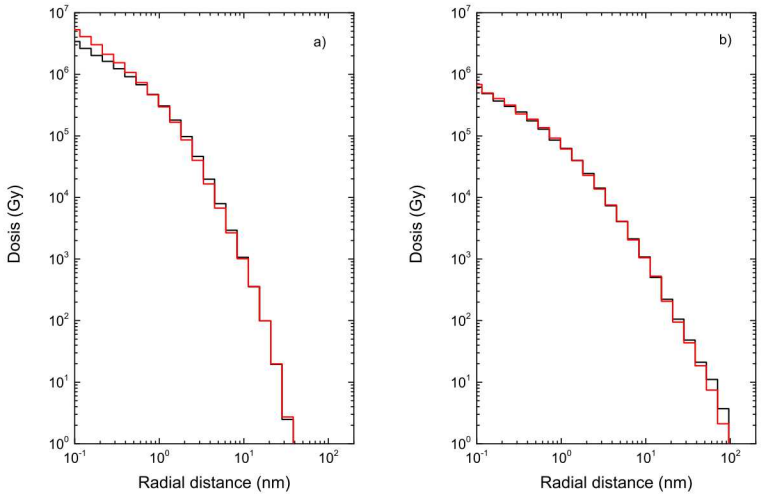

Figure 7: Comparison of radial dose profiles given by two incident proton energies, 100 keV (panel a) and 1 MeV (panel b). The secondary electron angular distribution are computed from theoretical mechanical-quantum (CDW-EIS) cross sections (red line) and from classical mechanics (back line).

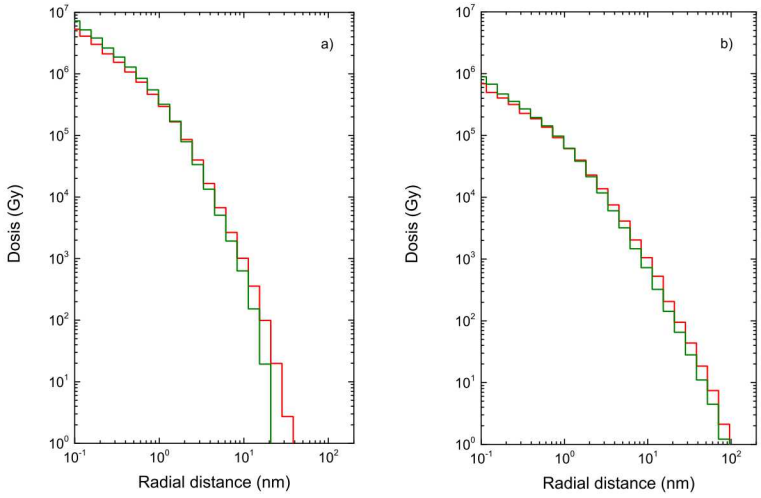

Figure 8: Comparison of radial dose profiles given by two incident proton energies, 100 keV (panel a) and 1 MeV (panel b), in vapor water (red line) and in hydrated DNA (green line).

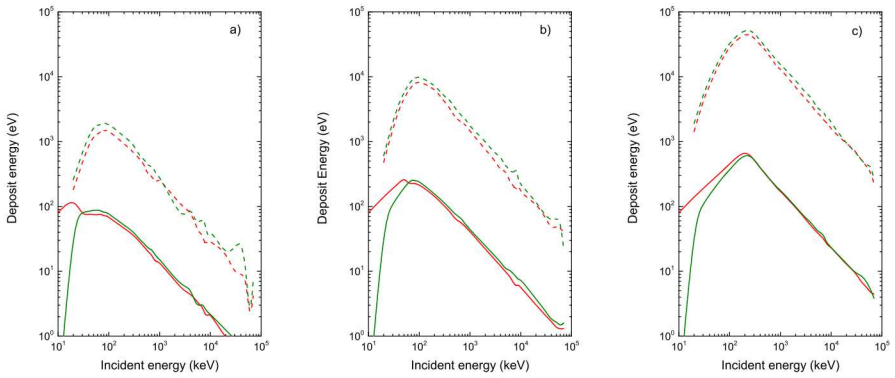

Figure 9: Energy deposition in cylinders (height × radius) of 2 × 1 nm (panel a), 10 × 2.5 nm (panel b) and 25 × 12.5 nm (panel c). Deposit energy by proton (solid line) and by secondary electrons (dashed line). Cylinders fill with water vapor (red lines) and hydrated DNA (green lines).

overview of the theoretical quantum mechanics CDW-EIS approximation used to characterize the ionizing processes, ionization and electron capture, induced by ions on vapor water and DNA nucleobases. We show theoretical predictions are able to reproduce the available experimental data for all the presented collisional systems. The computed theoretical cross sections have been used to build up the input database for the *TILDA-V* MCTS code. With the *TILDA-V* code, the micro-dosimetry endpoints were obtained for water and hydrated DNA, both for the primary and secondary particles, which have shown the importance of describing a realistic biological environment.

Acknowledgment

MAQ would likes to thank the Mésocentre de Calcul Intensif Aquitain (MCIA, Université de Bordeaux, Bordeaux, France) for the free computer time provided.

MAQ, JMM, CAT, OAF and RDD acknowledge financial support support from the Agencia Nacional de Promoción Científica y Tecnológica through the project PICT 2015-3392 institution from República Argentina.

Sandia National Laboratories is a multi-mission laboratory managed and

operated by National Technology and Engineering Solutions of Sandia, LLC., a wholly owned subsidiary of Honeywell International, Inc., for the U.S. Department of Energy's National Nuclear Security Administration under contract DE-NA0003525. The views expressed in the article do not necessarily represent the views of the U.S. Department of Energy or the United States Government.

References

[1] H. Nikjoo, D. Emfietzoglou, T. Liamsuwan, R. Taleei, D. Liljequist, S. Uehara, Radiation track, DNA damage and response - a review, Reports on Progress in Physics 79 (11) (2016) 116601. doi:10.1088/0034-4885/79/11/116601.

[2] S. Agostinelli, *et al.*, Geant4 simulation toolkit, Nuclear Instruments and Methods in Physics Research Section A: Accelerators, Spectrometers, Detectors and Associated Equipment 506 (3) (2003) 250 – 303. doi:10.1016/S0168-9002(03)01368-8.

[3] H. Iwase, K. Niita, T. Nakamura, Development of general-purpose particle and heavy ion transport monte carlo code, Journal of Nuclear Science and Technology 39 (11) (2002) 1142–1151. doi:10.1080/18811248.2002.9715305.

[4] A. Ferrari, P. R. Sala, A. Fassò, J. Ranft, Fluka : A multi-particle transport code, CERN (2005). doi:10.5170/CERN-2005-010.

[5] J. S. Hendricks, *et al.*, MCNPX, version 2.6. a, Los Alamos National Laboratory Report LA-UR-05-8225 (2005).

[6] W. Nelson, H. Hirayama, D. Rogers, The EGS4 code system, SLAC-Report-265 (1985).

[7] H. Nikjoo, S. Uehara, D. Emfietzoglou, F. A. Cucinotta, Track-structure codes in radiation research, Radiation Measurements 41 (2006) 1052–1074. doi:10.1016/j.radmeas.2006.02.001.

[8] B. Gervais, M. Beuve, G. H. Olivera, M. E. Galassi, R. D. Rivarola, Production of HO_2 and O_2 by multiple ionization in water radiolysis by swift carbon ions, Chemical Physics Letters 410 (2005) 330–334. doi:10.1016/j.cplett.2005.05.057.

[9] I. Plante, A Monte-Carlo step-by-step simulation code of the non-homogeneous chemistry of the radiolysis of water and aqueous solutions. Part I: theoretical framework and implementation, Radiation and Environmental Biophysics 50 (2011) 389–403. doi:10.1007/s00411-011-0367-8.

[10] W. Friedland, M. Dingfelder, P. Kundrt, P. Jacob, Track structures, DNA targets and radiation effects in the biophysical Monte Carlo simulation code PARTRAC, Mutation Research 711 (1) (2011) 28 – 40. doi:10.1016/j.mrfmmm.2011.01.003.

[11] W. Friedland, P. Jacob, H. G. Paretzke, T. Stork, Monte Carlo Simulation of the Production of Short DNA Fragments by Low-Linear Energy Transfer Radiation Using Higher-Order DNA Models, Radiation Research 150 (1998) 170. doi:10.2307/3579852.

[12] M. Bernal, D. Sikansi, F. Cavalcante, S. Incerti, C. Champion, V. Ivanchenko, Z. Francis, An atomistic geometrical model of the B-DNA configuration for DNAradiation interaction simulations, Computer Physics Communications 184 (12) (2013) 2840 – 2847. doi:10.1016/j.cpc.2013.07.015.

[13] M. A. Bernal, C. E. deAlmeida, S. Incerti, C. Champion, V. Ivanchenko, Z. Francis, The Influence of DNA Configuration on the Direct Strand Break Yield, Computational and Mathematical Methods in Medicine 417501. doi:10.1155/2015/417501.

[14] International Commission on Radiation Units Measurements, , Tech. Rep. ICRU Report 49, ICRU, Washington, DC, USA (1993).

[15] International Commission on Radiation Units Measurements, , Tech. Rep. ICRU Report 63, ICRU, Washington, DC, USA (2000).

[16] International Atomic Energy Agency Atomic and Molecular Data for Ra-

diation Therapy and Related Research, , Tech. Rep. IAEA-TECDOC-799, IAEA, Vienna, Austria (1995).

[17] M. E. Rudd, User-friendly model for the energy distribution of electrons from proton or electron collisions, International Journal of Radiation Applications and Instrumentation. Part D. Nuclear Tracks and Radiation Measurements 16 (2) (1989) 213 – 218. doi:10.1016/1359-0189(89)90052-6.

[18] J. P. Hansen, L. Kocbach, Ejection angles of fast delta electrons from K-shell ionisation induced by energetic ions, Journal of Physics B Atomic Molecular Physics 22 (1989) L71–L77. doi:10.1088/0953-4075/22/3/004.

[19] M. A. Bernal, J. A. Liendo, The HKS model for electron production in liquid water by light ions, Nuclear Instruments and Methods in Physics Research B 251 (2006) 171–176. doi:10.1016/j.nimb.2006.07.006.

[20] M. E. Rudd, T. V. Goffe, R. D. Dubois, L. H. Toburen, C. A. Ratcliffe, Cross sections for ionization of gases by 5 - 4000 keV protons and for electron capture by 5 - 150 keV protons, Physical Review A 28 (1983) 3244–3257. doi:10.1103/PhysRevA.28.3244.

[21] B. G. Lindsay, D. R. Sieglaff, K. A. Smith, R. F. Stebbings, Charge transfer of 0.5-, 1.5-, and 5-keV protons with H_2O: Absolute differential and integral cross sections, Physical Review A 55 (1997) 3945–3946. doi:10.1103/PhysRevA.55.3945.

[22] R. Dagnac, D. Blanc, D. Molina, A study on the collision of hydrogen ions H_1^+, H_2^+ and H_3^+ with a water-vapour target, Journal of Physics B Atomic Molecular Physics 3 (1970) 1239–1251. doi:10.1088/0022-3700/3/9/007.

[23] L. H. Toburen, M. Y. Nakai, R. A. Langley, Measurement of High-Energy Charge-Transfer Cross Sections for Incident Protons and Atomic Hy-

drogen in Various Gases, Physical Review 171 (1968) 114–122. doi:10.1103/PhysRev.171.114.

[24] M. Dingfelder, M. Inokuti, H. G. Paretzke, Inelastic-collision cross sections of liquid water for interactions of energetic protons, Radiation Physics and Chemistry 59 (2000) 255–275. doi:10.1016/S0969-806X(00)00263-2.

[25] I. Abbas, C. Champion, B. Zarour, B. Lasri, J. Hanssen, Single and multiple cross sections for ionizing processes of biological molecules by protons and α-particle impact: a classical Monte Carlo approach, Physics in Medicine and Biology 53 (2008) N41–N51. doi:10.1088/0031-9155/53/4/N03.

[26] H. Lekadir, I. Abbas, C. Champion, J. Hanssen, Total cross sections for ionizing processes induced by proton impact on molecules of biological interest: A classical trajectory Monte Carlo approach, Nuclear Instruments and Methods in Physics Research B 267 (2009) 1011–1014. doi:10.1016/j.nimb.2009.02.044.

[27] H. Lekadir, I. Abbas, C. Champion, O. Fojón, R. D. Rivarola, J. Hanssen, Single-electron-loss cross sections of DNA and RNA bases impacted by energetic multicharged ions: A classical Monte Carlo approximation, Physical Review A 79 (6) (2009) 062710. doi:10.1103/PhysRevA.79.062710.

[28] H. N. Tran, D. D. Dao, S. Incerti, M. A. Bernal, M. Karamitros, T. V. Nhan Hao, T. M. Dang, Z. Francis, Single electron ionization and electron capture cross sections for (C^{6+}, H_2O) interaction within the Classical Trajectory Monte Carlo (CTMC) approach, Nuclear Instruments and Methods in Physics Research B 366 (2016) 140–144. doi:10.1016/j.nimb.2015.10.017.

[29] C. Illescas, L. F. Errea, L. Méndez, B. Pons, I. Rabadán, A. Riera, Classical treatment of ion-H_2O collisions with a three-center model potential, Physical Review A 83 (5) (2011) 052704. doi:10.1103/PhysRevA.83.052704.

[30] T. Liamsuwan, H. Nikjoo, Cross sections for bare and dressed carbon ions in water and neon, Physics in Medicine & Biology 58 (3) (2013) 641. doi:10.1088/0031-9155/58/3/641.

[31] T. Liamsuwan, H. Nikjoo, A Monte Carlo track structure simulation code for the full-slowing-down carbon projectiles of energies 1 keV/u - 10 MeV/u in water, Physics in Medicine & Biology 58 (3) (2013) 673. URL http://stacks.iop.org/0031-9155/58/i=3/a=673

[32] H. J. Lüdde, T. Spranger, M. Horbatsch, T. Kirchner, Nonperturbative, quantum-mechanical approach to ion collisions from molecular targets, Physical Review A 80 (6) (2009) 060702. doi:10.1103/PhysRevA.80.060702.

[33] M. Murakami, T. Kirchner, M. Horbatsch, H. J. Lüdde, Single and multiple electron removal processes in proton-water-molecule collisions, Physical Review A 85 (5) (2012) 052704. doi:10.1103/PhysRevA.85.052704.

[34] M. Murakami, T. Kirchner, M. Horbatsch, H. J. Lüdde, Fragmentation of water molecules by proton impact: The role of multiple electron processes, Physical Review A 85 (5) (2012) 052713. doi:10.1103/PhysRevA.85.052713.

[35] M. Murakami, T. Kirchner, M. Horbatsch, H. J. Lüdde, Quantum-mechanical calculation of multiple electron removal and fragmentation cross sections in He^+-H_2O collisions, Physical Review A 86 (2) (2012) 022719. doi:10.1103/PhysRevA.86.022719.

[36] H. Luna, W. Wolff, E. C. Montenegro, A. C. Tavares, H. J. Lüdde, G. Schenk, M. Horbatsch, T. Kirchner, Ionization and electron-capture cross sections for single- and multiple-electron removal from H_2O by Li^{3+} impact, Physical Review A 93 (5) (2016) 052705. doi:10.1103/PhysRevA.93.052705.

[37] C. Champion, J. Hanssen, R. D. Rivarola, Chapter Ten - The First Born Approximation for Ionization and Charge Transfer in Energetic Collisions of Multiply Charged Ions with Water, in: D. Belki (Ed.), Theory of Heavy Ion Collision Physics in Hadron Therapy, Vol. 65 of Advances in Quantum Chemistry, Academic Press, 2013, pp. 269 – 313. doi:10.1016/B978-0-12-396455-7.00010-8.

[38] R. D. Rivarola, M. E. Galassi, P. D. Fainstein, C. Champion, Chapter Nine - Computation of Distorted Wave Cross Sections for High-Energy Inelastic Collisions of Heavy Ions with Water Molecules, in: D. Belki (Ed.), Theory of Heavy Ion Collision Physics in Hadron Therapy, Vol. 65 of Advances in Quantum Chemistry, Academic Press, 2013, pp. 231 – 267. doi:10.1016/B978-0-12-396455-7.00009-1.

[39] C. Champion, H. Lekadir, M. E. Galassi, O. Fojn, R. D. Rivarola, J. Hanssen, Theoretical predictions for ionization cross sections of DNA nucleobases impacted by light ions, Physics in Medicine & Biology 55 (20) (2010) 6053. doi:10.1088/0031-9155/55/20/002.

[40] M. E. Galassi, C. Champion, P. F. Weck, R. D. Rivarola, O. Fojón, J. Hanssen, Quantum-mechanical predictions of DNA and RNA ionization by energetic proton beams, Physics in Medicine and Biology 57 (2012) 2081–2099. doi:10.1088/0031-9155/57/7/2081.

[41] C. Champion, P. F. Weck, H. Lekadir, M. E. Galassi, O. A. Fojón, P. Abufager, R. D. Rivarola, J. Hanssen, Proton-induced single electron capture on DNA/RNA bases, Physics in Medicine and Biology 57 (2012) 3039–3049. doi:10.1088/0031-9155/57/10/3039.

[42] M. A. Quinto, J. M. Monti, P. D. Montenegro, O. A. Fojón, C. Champion, R. D. Rivarola, Single ionization and capture cross sections from biological molecules by bare projectile impact*, European Physical Journal D 71 (2017) 35. doi:10.1140/epjd/e2017-70652-6.

[43] M. A. Quinto, P. R. Montenegro, J. M. Monti, O. A. Fojón, R. D. Rivarola, Electron capture by swift ions from molecules of biological interest, Journal of Physics B Atomic Molecular Physics 51 (16) (2018) 165201. doi:10.1088/1361-6455/aad152.

[44] M. A. Quinto, J. M. Monti, P. F. Weck, O. A. Fojón, J. Hanssen, R. D. Rivarola, P. Senot, C. Champion, Monte Carlo simulation of proton track structure in biological matter, European Physical Journal D 71 (2017) 130. doi:10.1140/epjd/e2017-70709-6.

[45] K. Wiklund, G. H. Olivera, A. Brahme, B. K. Lind, Radial Secondary Electron Dose Profiles and Biological Effects in Light-Ion Beams Based on Analytical and Monte Carlo Calculations using Distorted Wave Cross Sections, Radiation Research 170 (2008) 83–92. doi:10.1667/RR0961.1.

[46] G. Bäckström, M. E. Galassi, N. Tilly, A. Ahnesjö, J. M. Fernández-Varea, Track structure of protons and other light ions in liquid water: Applications of the liontrack code at the nanometer scale, Medical Physics 40 (6Part1) (2013) 064101. doi:10.1118/1.4803464.

[47] M. Dingfelder, D. Hantke, M. Inokuti, H. G. Paretzke, Electron inelastic-scattering cross sections in liquid water, Radiation Physics and Chemistry 53 (1) (1998) 1 – 18. doi:10.1016/S0969-806X(97)00317-4.

[48] R. Garcia-Molina, I. Abril, S. Heredia-Avalos, I. Kyriakou, D. Emfietzoglou, A combined molecular dynamics and monte carlo simulation of the spatial distribution of energy deposition by proton beams in liquid water, Physics in Medicine & Biology 56 (19) (2011) 6475. doi:10.1088/0031-9155/56/19/019.

[49] R. N. Hamm, J. E. Turner, R. H. Ritchie, H. A. Wright, Calculation of heavy-ion tracks in liquid water, Radiation Research Supplement 8 (1985) S20–S26. doi:10.2307/3583507.

[50] M. Dingfelder, Updated model for dielectric response function of liquid water, Applied Radiation and Isotopes 83 (2014) 142 – 147. doi:10.1016/j.apradiso.2013.01.016.

[51] D. Emfietzoglou, I. Kyriakou, R. Garcia-Molina, I. Abril, H. Nikjoo, Inelastic cross sections for low-energy electrons in liquid water: Exchange and correlation effects, Radiation Research 180 (2013) 499– 513. doi:10.1667/RR13362.1.

[52] S. Endo, E. Yoshida, H. Nikjoo, S. Uehara, M. Hoshi, M. Ishikawa, K. Shizuma, A Monte Carlo track structure code for low energy protons, Nuclear Instruments and Methods in Physics Research B 194 (2002) 123–131. doi:10.1016/S0168-583X(02)00497-4.

[53] M. Zaider, D. J. Brenner, W. E. Wilson, The Applications of Track Calculations to Radiobiology I. Monte Carlo Simulation of Proton Tracks, Radiation Research 95 (1983) 231. doi:10.2307/3576252.

[54] S. Uehara, L. H. Toburen, H. Nikjoo, Development of a monte carlo track structure code for low-energy protons in water, International Journal of Radiation Biology 77 (2) (2001) 139–154. doi:10.1080/09553000010012536.

[55] T. Liamsuwan, S. Uehara, D. Emfietzoglou, H. Nikjoo, Physical and biophysical properties of proton tracks of energies 1 keV to 300 MeV in water, International Journal of Radiation Biology 87 (2) (2011) 141–160. doi:10.3109/09553002.2010.518204.

[56] S. Uehara, H. Nikjoo, Monte carlo track structure code for low-energy alpha-particles in water, The Journal of Physical Chemistry B 106 (42) (2002) 11051–11063. doi:10.1021/jp014004h.

[57] S. Incerti, *et al.*, Comparison of GEANT4 very low energy cross section models with experimental data in water, Medical Physics 37 (2010) 4692. doi:10.1118/1.3476457.

[58] M. Krämer, K. G., A Monte Carlo code for positive ion track simulation, Radiation and Environmental Biophysics 33 (1999) 91–109. doi:10.1007/BF01219334.

[59] D. Emfietzoglou, K. Karava, G. Papamichael, M. Moscovitch, Monte Carlo simulation of the energy loss of low-energy electrons in liquid water, Physics in Medicine and Biology 48 (2003) 2355–2371. doi:10.1088/0031-9155/48/15/308.

[60] W. E. Wilson, H. G. Paretzke, Calculation of Distributions for Energy Imparted and Ionization by Fast Protons in Nanometer Sites, Radiation Research 87 (1981) 521. doi:10.2307/3575518.

[61] S. M. Pimblott, J. A. LaVerne, A. Mozumder, N. J. B. Green, Structure of electron tracks in water. 1. Distribution of energy deposition events, The Journal of Physical Chemistry 94 (1) (1990) 488–495. doi:10.1021/j100364a084.

[62] J. E. Turner, J. L. Magee, H. A. Wright, A. Chatterjee, R. N. Hamm, R. H. Ritchie, Physical and Chemical Development of Electron Tracks in Liquid Water, Radiation Research 96 (1983) 437. doi:10.2307/3576111.

[63] F. Salvat, A generic algorithm for Monte Carlo simulation of proton transport, Nuclear Instruments and Methods in Physics Research B 316 (2013) 144–159. doi:10.1016/j.nimb.2013.08.035.

[64] W. Wilson, N. H., A Monte Carlo code for positive ion track simulation, Radiation and Environmental Biophysics 38 (1999) 97–104. doi:10.1007/s004110050144.

[65] V. Cobut, L. Cirioni, J. P. Patau, Accurate transport simulation of electron tracks in the energy range 1 keV-4 MeV, Nuclear Instruments and Methods in Physics Research B 215 (2004) 57–68. doi:10.1016/S0168-583X(03)01782-8.

[66] C. Champion, A. L'Hoir, M. F. Politis, P. D. Fainstein, R. D. Rivarola, A. Chetioui, A Monte Carlo Code for the Simulation of Heavy-Ion Tracks in Water, Radiation Research 163 (2005) 222–231. doi:10.1667/RR3295.

[67] R. D. Rivarola, R. D. Piacentini, A. Salin, D. Belkic, The influence of the static potential in high-energy K-shell electron capture collisions, Journal of Physics B Atomic Molecular Physics 13 (1980) 2601–2609. doi:10.1088/0022-3700/13/13/018.

[68] P. D. Fainstein, V. H. Ponce, R. D. Rivarola, A theoretical model for ionisation in ion-atom collisions. Application for the impact of multicharged projectiles on helium, Journal of Physics B Atomic Molecular Physics 21 (1988) 287–299. doi:10.1088/0953-4075/21/2/013.

[69] P. D. Fainstein, V. H. Ponce, R. D. Rivarola, Two-centre effects in ionization by ion impact, Journal of Physics B Atomic Molecular Physics 24 (1991) 3091–3119. doi:10.1088/0953-4075/24/14/005.

[70] N. Stolterfoht, R. D. DuBois, R. D. Rivarola, Electron Emission in Heavy Ion-Atom Collisions, Springer-Verlag Berlin Heidelberg, 1997.

[71] S. E. Corchs, R. D. Rivarola, J. H. McGuire, Impact-parameter formulation for electron capture from molecular targets, Physical Review A 47 (1993) 3937–3944. doi:10.1103/PhysRevA.47.3937.

[72] M. E. Galassi, R. D. Rivarola, P. D. Fainstein, Multicenter character in single-electron emission from H_2 molecules by ion impact, Physical Review A 70 (3) (2004) 032721. doi:10.1103/PhysRevA.70.032721.

[73] D. S. F. Crothers, J. F. McCann, Ionisation of atoms by ion impact, Journal of Physics B Atomic Molecular Physics 16 (1983) 3229–3242. doi:10.1088/0022-3700/16/17/015.

[74] D. Belkic, A quantum theory of ionisation in fast collisions between ions and atomic systems, Journal of Physics B Atomic Molecular Physics 11 (1978) 3529–3552. doi:10.1088/0022-3700/11/20/015.

[75] D. S. F. Crothers, Refined orthogonal variational treatment of continuum distorted waves, Journal of Physics B Atomic Molecular Physics 15 (1982) 2061–2074. doi:10.1088/0022-3700/15/13/022.

[76] J. M. Monti, O. A. Fojón, J. Hanssen, R. D. Rivarola, Single electron ionization of multishell atoms: dynamic screening and post-prior discrepancies in the CDW-EIS model, Journal of Physics B Atomic Molecular Physics 46 (14) (2013) 145201. doi:10.1088/0953-4075/46/14/145201.

[77] D. Belkić, R. Gayet, A. Salin, Electron capture in high-energy ion-atom collisions, Physics Reports 56 (1979) 279–369. doi:10.1016/0370-1573(79)90035-8.

[78] J. M. Monti, R. D. Rivarola, P. D. Fainstein, Distorted wave theories for dressed-ion-atom collisions with GSZ projectile potentials, Journal of Physics B Atomic Molecular Physics 44 (19) (2011) 195206. doi:10.1088/0953-4075/44/19/195206.

[79] P. P. Szydlik, A. E. Green, Independent-particle-model potentials for ions and neutral atoms with Z<=18, Physics Review. A 9 (1974) 1885–1894. doi:10.1103/PhysRevA.9.1885.

[80] R. H. Garvey, C. H. Jackman, A. E. S. Green, Independent-particle-model potentials for atoms and ions with 36 < Z <= 54 and a modified Thomas-Fermi atomic energy formula, Phycial Review A 12 (1975) 1144–1152. doi:10.1103/PhysRevA.12.1144.

[81] A. E. Martínez, G. R. Deco, R. D. Rivarola, P. D. Fainstein, K-Shell vacancy production in asymmetric collisions, Nuclear Instruments and Methods in Physics Research B 34 (1988) 32–36. doi:10.1016/0168-583X(88)90360-6.

[82] C. Champion, C. L. Loirec, B. Stosic, Epotran: A full-differential monte carlo code for electron and positron transport in liquid and gaseous water,

International Journal of Radiation Biology 88 (1-2) (2012) 54–61. doi:10.3109/09553002.2011.641451.

[83] C. Martin, , PhD thesis, University of Toulouse (2013).

[84] Perkins, S. T. and *et al.*, , Tech. Rep. Technical report UCRL-50400, 30, Lawrence Livermore National Laboratory, Livermore (1991).

[85] E. Clementi, C. Roetti, Roothaan-Hartree-Fock Atomic Wavefunctions: Basis Functions and Their Coefficients for Ground and Certain Excited States of Neutral and Ionized Atoms, Z <= 54, Atomic Data and Nuclear Data Tables 14 (1974) 177. doi:10.1016/S0092-640X(74)80016-1.

[86] K. Siegbahn, *et al.*, ESCA Applied to Free Molecules, Amsterdam: North-Holland, 1965.

[87] M. J. Frisch, *et al.*, Gaussian 90, Gaussian, Inc., Wallingford CT (2009).

[88] I. Abril, R. Garcia-Molina, C. D. Denton, I. Kyriakou, D. Emfietzoglou, Energy Loss of Hydrogen- and Helium-Ion Beams in DNA: Calculations Based on a Realistic Energy-Loss Function of the Target, Radiation Research 175 (2011) 247–255. doi:10.1667/RR2142.1.

[89] P. de Vera, R. Garcia-Molina, I. Abril, Angular and Energy Distributions of Electrons Produced in Arbitrary Biomaterials by Proton Impact, Physical Review Letters 114 (1) (2015) 018101. doi:10.1103/PhysRevLett.114.018101.

[90] J. A. LaVerne, S. M. Pimblott, Electron Energy-Loss Distributions in Solid, Dry DNA, Radiation Research 141 (1995) 208. doi:10.2307/3579049.

[91] Z. Tan, Y. Xia, M. Zhao, X. Liu, Proton stopping power in a group of bioorganic compounds over the energy range of 0.05 10 MeV, Nuclear Instruments and Methods in Physics Research B 248 (2006) 1–6. doi:10.1016/j.nimb.2006.04.073.

[92] G. D. Birnie, D. Rickwood, A. Hell, , Biochim. Biophys. Acta 331 (1973) 283.

[93] C. Champion, M. A. Quinto, J. M. Monti, M. E. Galassi, P. F. Weck, O. A. Fojón, J. Hanssen, R. D. Rivarola, Water versus DNA: new insights into proton track-structure modelling in radiobiology and radiotherapy, Physics in Medicine and Biology 60 (2015) 7805. doi:10.1088/0031-9155/60/20/7805.

[94] L. H. Toburen, W. E. Wilson, Energy and angular distributions of electrons ejected from water vapor by 0.3?1.5 mev protons, The Journal of Chemical Physics 66 (11) (1977) 5202–5213. doi:10.1063/1.433783.

[95] D. Ohsawa, Y. Sato, Y. Okada, V. P. Shevelko, F. Soga, 6.0-10.0-MeV/u He^{2+} -ion-induced electron emission from water vapor, Physical Review A 72 (6) (2005) 062710. doi:10.1103/PhysRevA.72.062710.

[96] D. Ohsawa, H. Tawara, F. Soga, M. E. Galassi, R. D. Rivarola, 6.0 MeV u^{-1} carbon ion (C^{6+} and C^{4+})-induced secondary electron emission from water vapor, Physica Scripta Volume T 156 (1) (2013) 014039. doi:10.1088/0031-8949/2013/T156/014039.

[97] S. Nandi, S. Biswas, A. Khan, J. M. Monti, C. A. Tachino, R. D. Rivarola, D. Misra, L. C. Tribedi, Double-differential cross sections for ionization of H_2O by fast bare O ions: Comparison with continuum-distorted-wave eikonal-initial-state calculations in prior and post forms, Physical Review A 87 (5) (2013) 052710. doi:10.1103/PhysRevA.87.052710.

[98] Y. Iriki, Y. Kikuchi, M. Imai, A. Itoh, Absolute doubly differential cross sections for ionization of adenine by 1.0-MeV protons, Physical Review A 84 (3) (2011) 032704. doi:10.1103/PhysRevA.84.032704.

[99] A. N. Agnihotri, S. Kasthurirangan, S. Nandi, A. Kumar, C. Champion, H. Lekadir, J. Hanssen, P. F. Weck, M. E. Galassi, R. D. Rivarola, O. Fojón, L. C. Tribedi, Absolute total ionization cross sections of uracil

($C_4H_4N_2O_2$) in collisions with MeV energy highly charged carbon, oxygen and fluorine ions, Journal of Physics B Atomic Molecular Physics 46 (18) (2013) 185201. doi:10.1088/0953-4075/46/18/185201.

[100] M. E. Rudd, T. V. Goffe, R. D. Dubois, L. H. Toburen, Cross sections for ionization of water vapor by 7-4000-keV protons, Physical Review A 31 (1985) 492–494. doi:10.1103/PhysRevA.31.492.

[101] A. C. Tavares, H. Luna, W. Wolff, E. C. Montenegro, Double ionization of water molecules induced by swift protons, Physical Review A 92 (3) (2015) 032714. doi:10.1103/PhysRevA.92.032714.

[102] M. A. Bolorizadeh, M. E. Rudd, Angular and energy dependence of cross sections for ejection of electrons from water vapor. II. 15-150-keV proton impact, Physical Review A 33 (1986) 888–892. doi:10.1103/PhysRevA.33.888.

[103] M. E. Rudd, T. V. Goffe, A. Itoh, Ionization cross sections for 10-300-keV/u and electron-capture cross sections for 5-150-keV/u $^3He^{2+}$ ions in gases, Physical Review A 32 (1985) 2128–2133. doi:10.1103/PhysRevA.32.2128.

[104] L. H. Toburen, W. E. Wilson, R. J. Popowich, Secondary Electron Emission from Ionization of Water Vapor by 0.3- to 2.0-MeV He^+ and He^{2+} Ions, Radiation Research 82 (1980) 27. doi:10.2307/3575234.

[105] P. S. Rudolph, C. E. Melton, Experimental and Theoretical Considerations for Ionization of Simple Hydrocarbons, H_2, D_2, O_2, H_2O, and the Rare Gases by 2.2-MeV α Particles and by Electrons in a Mass Spectrometer, Journal of Chemical Physics 45 (1966) 2227–2232. doi:10.1063/1.1727915.

[106] T. Liamsuwan, H. Nikjoo, Cross sections for bare and dressed carbon ions in water and neon, Physics in Medicine and Biology 58 (2013) 641. doi:10.1088/0031-9155/58/3/641.

[107] F. Gobet, B. Farizon, M. Farizon, M. J. Gaillard, M. Carré, M. Lezius, P. Scheier, T. D. Märk, Total, Partial, and Electron-Capture Cross Sections for Ionization of Water Vapor by 20-150 keV Protons, Physical Review Letters 86 (2001) 3751–3754. doi:10.1103/PhysRevLett.86.3751.

[108] C. L. Wingate, J. W. Baum, Measured Radial Distributions of Dose and LET for Alpha and Proton Beams in Hydrogen and Tissue-Equivalent Gas, Radiation Research 65 (1) (1976) 1–19. doi:10.2307/3574282.

[109] G. H. Olivera, P. D. Fainstein, R. D. Rivarola, Contribution from the inner shell of water vapour to dose profiles under proton and alpha particle irradiation, Physics in Medicine & Biology 41 (9) (1996) 1633. doi:10.1088/0031-9155/41/9/005.

[110] J. J. Butts, R. Katz, Theory of RBE for Heavy Ion Bombardment of Dry Enzymes and Viruses, Radiation Research 30 (4) (1967) 855–871. doi:10.2307/3572151.

[111] P. Olko, J. Booz, H. G. Paretzke, W. E. Wilson, Energy deposition in nanometer sites based on the track structure calculations., in: Atomic and Molecular Data for Radiotherapy, IAEA, Vienna, 1989, pp. 105–116.

[112] D. Emfietzoglou, K. Karava, G. Papamichael, M. Moscovitch, Monte-Carlo Calculations of Radial Dose and Restricted-LET for Protons in Water, Radiation Protection Dosimetry 110 (2004) 871–879. doi:10.1093/rpd/nch163.